A viscoelastic approach to the modelling of the transient closure behaviour of tabular excavations after blasting

by D.F. Malan*

Synopsis

This study investigates transient closure profiles of tabular excavations. Measured closure profiles in stopes indicate that time-dependent effects of the rockmass can be very prominent, but such effects have been largely neglected in past analyses and modelling. This was due to a poor understanding of the time-dependent mechanisms controlling closure rates. This paper investigates the feasibility of representing the rockmass as a visco-elastic medium. Currently, no analytical solution for the viscoelastic convergence of a tabular stope is available in the literature. Therefore, the author derived a solution using the correspondence principle and a known elastic solution. It is assumed that the rockmass behaves elastically in hydrostatic compression and as a Kelvin substance in distortion. A parametric study is included to aid in the calibration of the model parameters, together with a discussion on the correct calibration of these parameters from experimental data.

* *Miningtek Division, CSIR, P.O. Box 91230, Auckland Park, 2006 Gauteng.*

 SA ISSN 0038-223X/3.00 + 0.00. Paper received Dec. 1994; revised paper received May 1995.

Introduction

Most studies directed at the rock mechanics aspects of tabular excavations have assumed that the surrounding rockmass can be represented by a linear elastic medium[1]. This assumption also forms the basis of several simulation programs used throughout the South African mining industry[2,3]. This assumption is based on early investigations and does indeed provide an acceptable description of the behaviour of the rock in certain situations[4-6]. However, it is well known that there are discrepancies between elastic theory and actual rock behaviour that are especially noticeable in the immediate vicinity of an excavation. This is partly because of the inelastic behaviour of the broken rock and partly because of the time-dependent properties of the rock. In this paper, the term *time dependency* is taken to refer to deformation that is not related to geometric changes in the dimensions of an excavation and that occurs on a time scale of hours or days, i.e. the deformation is not related to elastodynamic seismic behaviour.

To avoid confusion, the terms *convergence, closure,* and *viscoelastic convergence* need to be defined. Following Gürtunca and Adams[7], *convergence* refers to the elastic component of closure. Inelastic closure with elastic convergence together form *closure*. For the purpose of this study, the time-dependent movement is added as a third component of closure. *Viscoelastic convergence* is the relative hangingwall and footwall movements predicted for an idealized stope in a continuum viscoelastic medium.

Gürtunca *et al.*[8] and Gürtunca and Adams[7] investigated the discrepancy between the measured closure values in stopes and the elastic convergence predicted by MINSIM-D. It was found that the closure can be several times larger than the elastic convergence. It was suggested that the closure measured underground has three components: elastic convergence, inelastic bed separations, and closure due to dilation. Dilation ahead of the mining faces, due to extension fracturing and shear movements, generates horizontal stresses, which cause the strata to deform into the stope, increasing the closure. To account for the inelastic behaviour, Gürtunca and Adams[7] suggested the use of an effective modulus in elastic computer modelling. Another approach in the modelling of inelastic behaviour is the use of special computer programs capable of simulating inelastic rock movements. These programs employ techniques such as the distinct-element method[9] or the displacement discontinuity method[10].

The other important component of closure, namely time-dependent behaviour of the rockmass, was largely neglected in past analyses owing to the difficulty of incorporating time effects in models. This problem needs to be addressed to enable engineers to predict the long-term stability of service excavations. A knowledge of time-dependent components will also lead to more accurate prediction of closure in stopes. Curran and Crawford[11] represented time-dependent effects in rock as having two components: the creep of intact rock and the creep along discontinuities. However, the relative importance of these two components is not well understood and needs to be investigated further.

This paper investigates the transient closure (which is a function of all the components already described) in stopes after blasting. The term *transient closure* is understood to mean the closure as a function of time observed between successive blasting operations. It must therefore be emphasized that there are no changes in the excavation geometry in the study of transient-closure behaviour. A number of workers[8,12] have studied closure in stopes as a function of face advance or number of days. These studies included the complicating effect of changes in geometry, which are not considered in the present study. It should be noted, however, that the closure observed for a face left standing can be regarded as transient behaviour since no changes in the geometry take place after the blasting operation. The following noteworthy studies of transient-closure behaviour are described in the literature.

Leeman[13] used closure recorders to measure transient-closure profiles in a tabular stope at East Rand Proprietary Mines. He observed profiles similar to Figure 1, in which the rate of closure suddenly increases just after blasting time. This high rate of closure decreases within hours to give a gradual asymptotic closure until the next blast occurs and the pattern is repeated. Similar closure profiles were observed at other mines in South Africa[14,15]. However, Leeman did not give any explanation for the observed closure profiles, although he did note that the amount of closure caused by blasting diminishes with distance from the working face. The rate of closure also varied greatly from one point to the next, and was affected by the position of the measuring point in relation to the support in the stope.

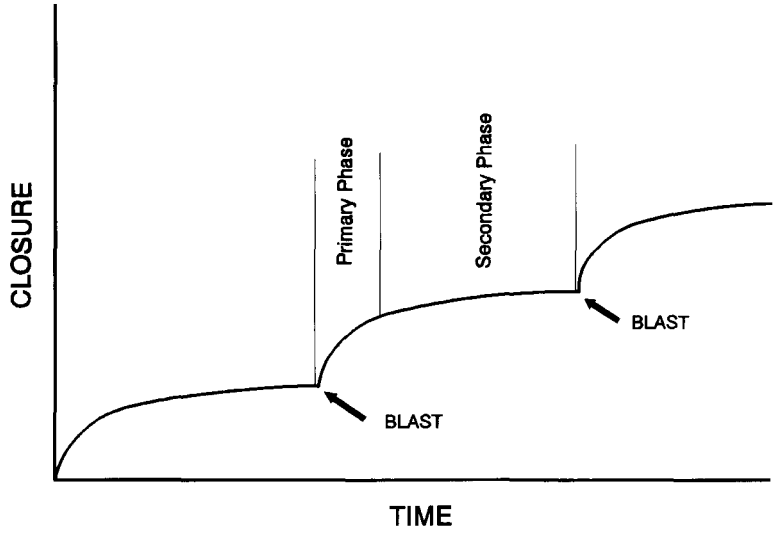

Figure 1—Typical profile of continuous stope closure as a function of time

Hodgson[16] also took closure measurements in East Rand Proprietary Mines. He explained the gradual asymptotic closure as being caused by the time-dependent migration of the fracture zone ahead of the face, resulting in the effective span becoming larger. He predicted that, if the face advanced faster than the migration of the fracture zone, less energy would be released in a stable manner, thereby increasing the incidence of rockbursts. This is in agreement with the statistical analysis of Cook *et al.*[4], which indicated an increase in rockbursts for a face advance rate of more than 4 m a month for small abutments to 8 m a month for large abutments.

The first quantitative attempt to analyse the transient-closure profiles of tabular stopes was made by McGarr[17] using data from East Rand Proprietary Mines. He used an empirical approach to represent the closure, δ:

$$\delta = \frac{B}{C}\sum_{n=0,n\neq 7m}^{\infty}\left(1-e^{-DC(t-24n)}\right)H(t-24n), \quad [1]$$

where B, C, and D are positive constants, n and m are integers, and H is the Heaviside unit function (H(t) = 1 for $t \geq 0$ and 0 for $t < 0$). The unit of time t in the equation is hours. At the time of McGarr's study, no blasting was allowed on Sundays and $n = 7$ m corresponds to those days. The rate of closure is obtained from equation [1] by differentiating:

$$\dot{\delta} = DB\sum_{n=0,n\neq 7m}^{\infty} e^{-DC(t-24n)}H(t-24n). \quad [2]$$

After the last blasting period of the week on Saturday, the closure and the rate of closure become

$$\delta = a\left(1-e^{-\frac{t}{\tau}}\right) \quad [3]$$

and

$$\dot{\delta} = be^{-\frac{t}{\tau}} \quad [4]$$

respectively, where a and b are constants and $\tau = 1/DC$. McGarr[17] suggested that the relaxation time, τ, can be used as a parameter to describe the ability of the rockmass to form a fracture zone in response to face advance. High values of τ might be associated with mines that are prone to rockbursts.

Kersten[14] analysed continuous closure profiles using data from Hartebeesfontein Gold Mine. He expressed the data on a log–log basis and used the following empirical formulation for the transient closure behaviour:

$$\log(s) = m\log(h) + \log(F), \quad [5]$$

where

s = closure
m = slope of the curve
h = hours
F = a constant.

He suggested that there is a possible link between the frequency of seismic activity and the time constants in the convergence data. As mentioned earlier, this was also suggested by McGarr[17], and warrants further investigation.

Although these empirical approaches are a useful representation of the experimental data, they are difficult to use as a prediction tool in other stopes where the governing parameters (e.g. span, dip, stress, incremental face advance) are different. Therefore, a theoretical approach is used in this paper that is based on an idealized viscoelastic model of the rockmass.

Following the above discussion, the transient closure of any tabular excavation is a function of the superposition of the following factors:

- elastic convergence of the rock
- inelastic closures caused by existing discontinuities (fractures, joints, and bedding planes)
- creep of the intact rock
- creep along existing discontinuities
- time-dependent formation of new fractures and resulting inelastic movements.

It is very difficult to quantify the amount of closure contributed by each component. This paper investigates the feasibility of representing the rockmass surrounding tabular excavations as an equivalent viscoelastic medium that includes all the factors mentioned above. Although the contributions of the individual components cannot be distinguished, this approach enables time-dependent effects that occur independently of the geometrical changes to the stope to be modelled. It must, however, be borne in mind that the contribution of inelastic movements and creep along discontinuities is more pronounced in the skin of the excavation than in the intact rock further away from the excavation. The first-order assumption of a continuum viscoelastic medium ignores this effect. If the viscoelastic parameters are calibrated from skin-to-skin closure measurements, the calibrated values are valid only in this region.

Viscoelastic convergence in a parallel-sided panel

Currently, no analytical solution for the viscoelastic convergence of a tabular stope without contact between the hangingwall and the footwall is available in the literature. The author therefore derived a solution using the correspondence principle of viscoelasticity and two building blocks: namely, a known elastic solution and a certain viscoelastic model.

The correspondence principle is a technique used to obtain viscoelastic solutions when the solution to the problem in the elastic domain is known[18]. It was used by Salamon[1] and Pan and Dong[19] to calculate the time-dependent convergence of a circular tunnel. The principle states that the Laplace transform of the solution can be found by replacement of the elastic constants (bulk and shear modulus or Young's modulus and Poisson's ratio) and the loads in the elastic solution by their Laplace transforms. The Laplace transforms of the elastic constants will look different for the various viscoelastic models. The solution in the time domain can then be found by the taking of the inverse Laplace transform.

Obtaining the first building block is trivial since Salamon[20] derived the elastic solution for the convergence in a parallel-sided panel where there is no contact between the hangingwall and the footwall.

Viscoelasticity models can be built from simple elements: namely, elastic elements or springs and viscosity elements or dashpots[18]. Three models used frequently are the Maxwell model comprising a spring and dashpot in series, the Kelvin model comprising a spring and dashpot in parallel, and the three-parameter solid in which an additional spring is placed in series with the Kelvin model (Figure 2).

When a constant stress is applied to the models, the following behaviour is noted[18].

- The *Maxwell model* experiences an instantaneous strain, followed by a linearly increasing strain.
- For the *Kelvin model,* the strain is zero at the time of stress application and then increases, approaching an asymptotic value exponentially.
- The *three-parameter solid* behaves similarly to the Kelvin model, but differs in the fact that it displays an instantaneous strain.

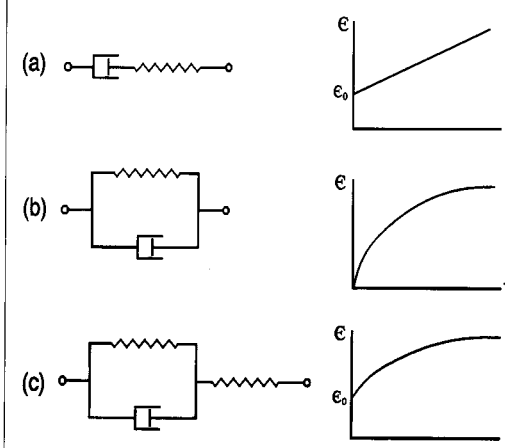

Figure 2—Models for the (a) Maxwell material, (b) Kelvin material, and (c) three-parameter solid. The diagrams of strain (ε) versus time (t) illustrate the behaviour of each model when subjected to a constant stress

Figure 1 shows that the closure of tabular stopes approaches an asymptotic value after the excavation is enlarged. This behaviour can therefore be modelled by both the Kelvin model and the three-parameter solid. McGarr[17] provided data and an analysis illustrating that the instantaneous closure at the time of face advance is negligible, and that the eventual closure is associated almost entirely with the time-dependent migration of the fracture zone ahead of the face. Data supplied by Güler[15] and closure profiles published by Leeman[13] confirm the statement that the instantaneous closure at the time of face advance is negligible compared with the eventual closure. Therefore, when the equation for viscoelastic convergence was obtained in the present study, the Kelvin model with no instantaneous strain components was used as a building block. However, it is important to emphasize that it is not known whether this assumption is applicable to all geotechnical areas throughout the mining industry. More experimental work is necessary to address this question. To allow for the possible scenario where instantaneous closure is significant, the relevant equations with the three-parameter solid as building block are given in the Addendum.

When the correspondence principle is applied to Salamon's elastic solution and it is assumed that the rock behaves elastically in hydrostatic compression and as a two-parameter Kelvin substance in distortion, the following viscoelastic convergence equation is obtained. (This equation cannot be found in the currently available literature and, as derived by the author, is given in the Addendum.)

$$S_z(x,t) = -4W_z\sqrt{l^2-x^2}\left(1+\frac{dx}{2}\right)g\left[1+c_1e^{-a_1t}-(c_1+1)e^{-a_2t}\right], \quad [6]$$

$$W_z = \frac{-\gamma H}{2}\left[(1+k)+(1-k)\cos 2\alpha\right] \quad [7]$$

$$d = \frac{\sin\alpha\cos\beta}{H} \quad [8]$$

$$g = \frac{3K+2q_0}{q_0(6K+q_0)} \quad [9]$$

$$a_1 = \frac{q_0}{q_1} \quad [10]$$

$$a_2 = \frac{6K+q_0}{q_1} \quad [11]$$

$$c_1 = -\frac{6K+q_0}{6K+4q_0}, \quad [12]$$

where

S_z = viscoelastic convergence
l = half span of the stope
x = distance from the centre of the stope (origin of co-ordinate system)
γ = specific weight of the rock
H = depth below surface
k = ratio of horizontal to vertical stress
α = dip of the reef
β = angle between x-axis and dip
K = bulk modulus
q_0 = $2G$, where G is the shear modulus
q_1 = viscosity coefficient of the viscous element in the two-parameter Kelvin model
g = compliance function
a_1 = secondary time constant
a_2 = primary time constant
c_1 = a viscoelastic parameter determining the slope of the secondary convergence phase.

The z-axis is perpendicular to the plane of the excavation and points towards the footwall. The two-dimensional section is taken parallel to a plane normal to the y-axis[21] (Figure 3).

It is clear from equations [9] to [12] that the viscoelastic parameters g, c_1, a_1, and a_2 are not fundamental material constants but functions of the bulk modulus, shear modulus, and viscosity coefficient. These parameters are grouped together as g, c_1, a_1, and a_2 to simplify the calibration of the parameters when experimental closure data are used. The bulk and shear modulus can be obtained from the calibrated parameters by the solving of the two simultaneous equations [9] and [12] to give

$$K = \frac{4c_1+1}{12gc_1(1+c_1)} \quad [13]$$

$$G = \frac{-1}{4gc_1}. \quad [14]$$

This can be written in terms of Young's modulus, E, and Poisson's ratio, ν, as

$$E = \frac{4c_1+1}{-4gc_1^2} \quad [15]$$

$$\nu = \frac{2c_1+1}{2c_1}. \quad [16]$$

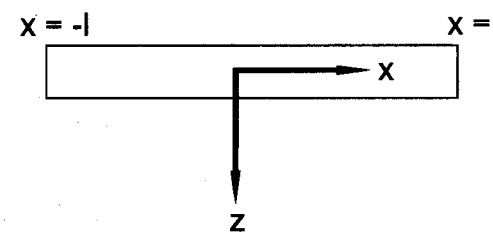

Figure 3—Co-ordinate system used in the viscoelastic convergence model

The viscosity coefficient, q_1, can be obtained by substitution of equation [14] into [10] to give

$$q_1 = \frac{1}{-2gc_1a_1}. \qquad [17]$$

As the viscosity coefficient can be obtained from either equation [10] or [11], it follows that the time constants a_1 and a_2 are not independent. Equations [10] and [11] can be combined if q_1 is eliminated and equations [13] and [14] are substituted to give the relationship between the time constants as

$$a_1 = a_2\frac{(1+c_1)}{-3c_1}. \qquad [18]$$

When $t \to \infty$, the viscoelastic convergence approaches an asymptotic value given by

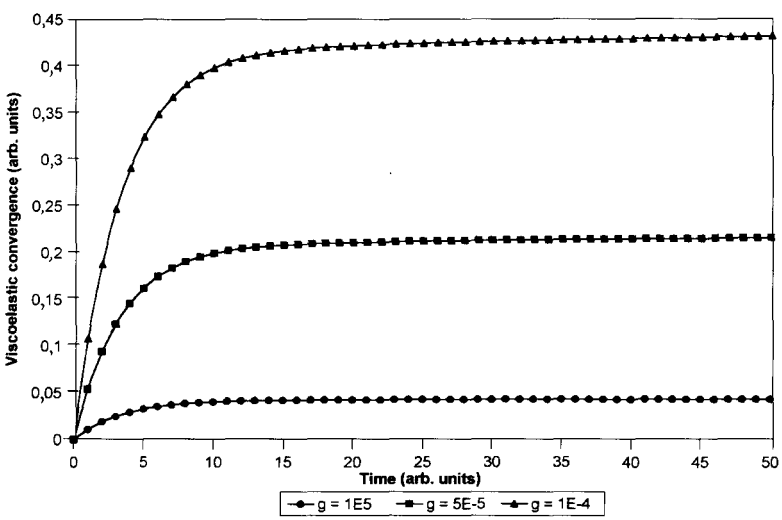

Figure 4—The effect of the compliance, g, on the viscoelastic convergence. The curves were calculated for c_1 = –0,1, α_1 = 0,01, and α_2 = 0,3

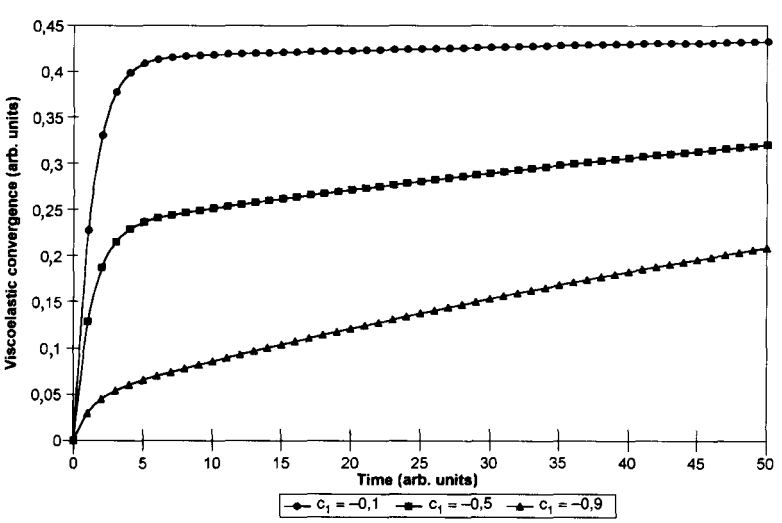

Figure 5—The effect of the secondary slope constant, c_1, on the viscoelastic convergence. The curves were calculated for g = –0,0001, α_1 = 0,01, and α_2 = 0,3

$$S_z(x) = -4W_z g\sqrt{l^2 - x^2}\left(1 + \frac{dx}{2}\right). \qquad [19]$$

The only viscoelastic parameter present in equation [19] is g. It follows from the definition of g in equation [9] that it is only a function of the bulk and shear modulus. The magnitude of the viscoelastic convergence when $t \to \infty$ is therefore not dependent on the viscosity coefficient. It can easily be shown that, when $t \to \infty$, the viscoelastic solution is identical to the elastic solution by substitution of equation [9] into equation [19] and rewriting of the bulk and shear modulus in terms of Young's modulus and Poisson's ratio. (The elastic solution is given as equation [A1] in the Addendum.)

The length of span L_c at which there is contact between the hangingwall and the footwall at the centre of the stope ($x = 0$) at time $t \to \infty$ is

$$L_c = 2l = \frac{S_z}{-2W_z g\left(1 + \frac{dx}{2}\right)}, \qquad [20]$$

with S_z set equal to the stoping width.

In the study of the time-dependent behaviour of materials, curves are usually divided into primary, secondary, and tertiary regimes[22]. Data on stope closure also display typical primary and secondary behaviour, as illustrated in Figure 1. To aid the fit of experimental data, knowledge of the effect of the parameters g, c_1, a_1, and a_2 on the two viscoelastic convergence phases is needed, and a parametric study was therefore conducted. The parameter g, or the compliance, determines the magnitude of the viscoelastic convergence but not the convergence rate in the primary or secondary phase (Figure 4). An excavation in rock with a high value of g will therefore experience a larger closure at any instant of time than a similar excavation in rock with a smaller value of g. Parameter c_1 determines the viscoelastic convergence rate of the secondary phase, as well as the magnitude of the viscoelastic convergence in this phase (Figure 5).

It follows from equation [18] that the time constants a_1 and a_2 are not independent. For the purpose of the parametric study, they were considered independent to illustrate the individual regions of influence more clearly (e.g. a_1 was kept constant while a_2 was varied). However, when closure data are calibrated, the relationship given in equation [18] needs to be maintained. Figure 6 illustrates the strong dependency of the viscoelastic convergence rate in the primary phase on parameter a_2, and this is subsequently referred to as the primary time constant.

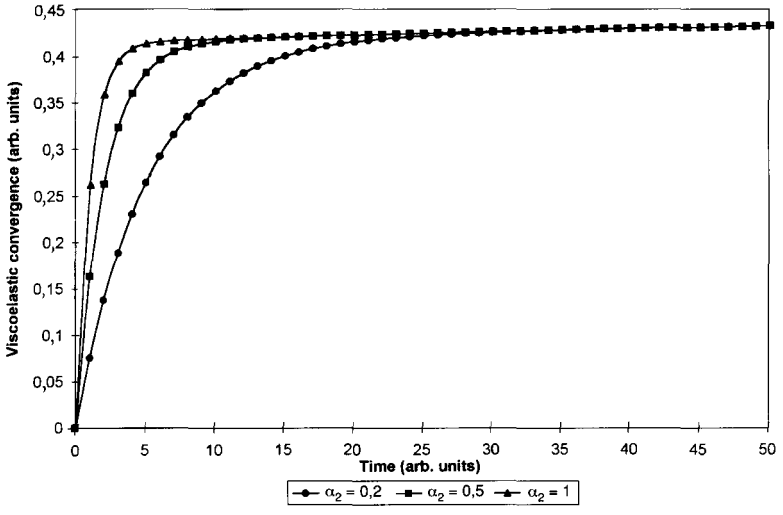

Figure 6—The effect of the primary time constant, α_2, on the viscoelastic convergence. The curves were calculated for g = –0,0001, c_1 = –0,1, and α_1 = 0,01

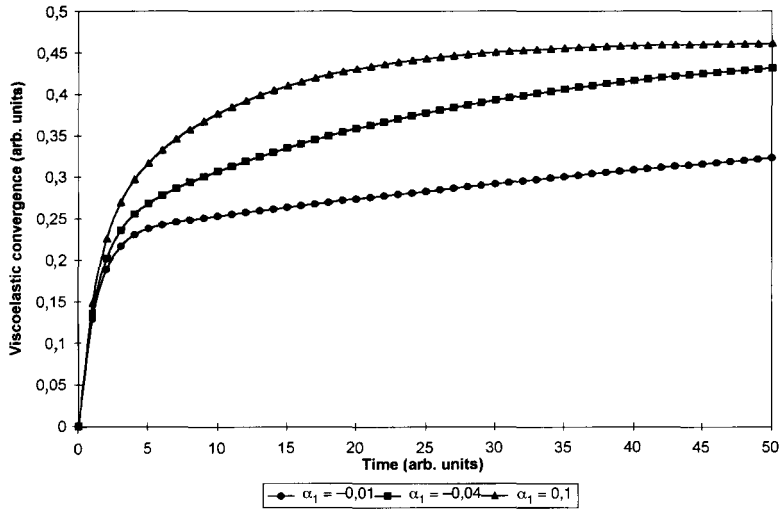

Figure 7—The effect of the secondary time constant, α_1, on the viscoelastic convergence. The curves were calculated for g = –0,0001, c_1 = –0,5, and α_2 = 0,3

Parameter a_1, or the secondary time constant, affects the rate at which the viscoelastic convergence in the secondary phase approaches the asymptotic value, as illustrated in Figure 7.

Incremental face advance

Equation [6] is applicable to situations where the total length of the stope is excavated instantaneously. This is not the case in practice, where the face is advanced incrementally. If it is assumed that the first mining increment is created suddenly at time τ_1, giving a stope of half span L, equation [6] will give the viscoelastic convergence for this step as $S_z(l = L,x,t, -\tau_1)$. At time τ_2, the face is advanced on both sides of the stope by Δl, giving a half span of $L + \Delta l$.

Equation [6] with a half span of $L + \Delta l$ at time τ_2 results in the total span being created in one step, which is clearly wrong. At time $\tau_2 + \Delta\tau$, the total viscoelastic convergence is the sum of the viscoelastic convergence caused by a half span of L (excavated at time τ_1) plus an incremental viscoelastic convergence caused by the incremental length Δl (excavated at time τ_2). The incremental viscoelastic convergence is the difference between the viscoelastic convergence of a stope with half span $L + \Delta l$ created at time τ_2 and the viscoelastic convergence of a stope with half span L also created at time τ_2. Therefore, at time $\tau_2 + \Delta\tau$, the viscoelastic convergence is given as

$$S_z = S_z(l = L,x,t-\tau_1) + S_z(l = L + \Delta l,x,t-\tau_2) - S_z(l = L,x,t-\tau_2). \quad [21]$$

Salamon[1] used arguments of negative and positive superposition to give a general expression for an arbitrarily shaped excavation created in n increments:

$$u = \left\{\sum_{i=1}^{n-1}\left[F_i(l_i,t-\tau_i)\right]-\left[F_i(l_i,t-\tau_{i+1})\right]\right\} + F_n\left[l_n,t-\tau_n\right], \quad [22]$$

which is valid for

$$\tau_n < t < \tau_{n+1},$$

where

- u = a displacement component at some point in the rock
- F_i = some function dependent on the shape of the excavation
- l_i = a critical linear dimension of the excavation.

If the shape of the excavation stays constant, ($F_1 = F_2 = F$) and $n = 2$, then equation [22] is reduced to equation [21] with $F = S_z$.

Parameter calibration from stope-closure data

Instruments to measure closure are usually installed in stopes where the span has already reached a significant length. Although an appreciable amount of closure has taken place up to the time of installation, the amount is unknown, and the closure is therefore taken to be zero at this point for a reference level. It is therefore not possible to calibrate the model with the number of steps, since the incremental advance for every step and the increase in closure for every step are unknown. However, if the span is increased by blasting, the incremental closure can be used to calibrate g, c_1, a_1, and a_2. The incremental viscoelastic convergence can be obtained from equation [21] if the first term is set equal to zero:

$$\Delta S_z = S_z(l = L + \Delta l,x,t-\tau_2) - S_z(l = L,x,t-\tau_2). \quad [23]$$

Acknowledgements

This work forms part of the rockmass behaviour research programme of Rock Engineering, CSIR Division of Mining Technology. The author acknowledges the financial assistance and support received from the Safety in Mines Research Advisory Committee (SIMRAC). The author is working towards a Ph.D. degree at the University of the Witwatersrand, and the work described here also forms part of that study. R.W.O. Kersten initiated this study by supplying data that had not previously been published and by emphasizing the importance of studying time-dependent behaviour. G. Güler is thanked for supplying unpublished data. The author also thanks Drs J.A.L. Napier, N.C. Gay, and R.G. Gürtunca, and an anonymous referee for reviewing the manuscript and making several useful comments.

References

1. SALAMON, M.D.G. Rock mechanics of underground excavations. *Proceedings 3rd Congress of the International Society for Rock Mechanics.* 1974. pp. 951–1099.

By substitution of equation [6] on the assumption that the stress before and after the blast stays the same,

$$\Delta S_z(x,t) = -4W_z\left(1+\frac{dx}{2}\right)g \left[1+c_1e^{-a_1t}-(c_1+1)e^{-a_2t}\right] \left[\sqrt{(L+\Delta l)^2-x^2}-\sqrt{L^2-x^2}\right]. \quad [24]$$

In Figure 8, the incremental viscoelastic convergence, ΔS_z (equation [24]), is plotted as a function of the distance from the face for a stope with a half span of 50 m and a face advance of 1 m. (Arbitrary values were used for the parameters t, W_z, g, c_1, a_1, a_2, with x ranging from L to 0.) It follows from Figure 8 that, the further the point of measurement from the face, the less the incremental viscoelastic convergence following every blast. This is in agreement with Leeman's observation[13] that the effect of blasting upon closure becomes progressively less as the point of measurement becomes further from the working face. Ideally for more accurate calibration of the parameter, the measurement station should be installed close to the face to give a large incremental closure.

Equation [24] assumes that both sides of the stope are blasted simultaneously, giving an advance of Δl at both faces. However, this is seldom the case in underground workings, where only one side of the panel is often blasted. This problem is solved by the introduction of an equivalent stope principle. Equation [24] is based on both linear elasticity theory and linear viscoelasticity theory, and therefore an advance of Δl on one side only (Figure 9a) can be represented by an equivalent stope with a simultaneous advance of $\Delta l/2$ on both sides, provided that the measuring point is shifted by a distance of $\Delta l/2$ away from the blasted face to keep the original distance to the face (length a) the same (Figure 9b). For a stope with a face advance of Δl at one side only, equation [24] can therefore be written as

$$\Delta S_z(x,t) = -4W_z\left(1+\frac{dx}{2}\right)g \left[1+c_1e^{-a_1t}-(c_1+1)e^{-a_2t}\right] \left[\sqrt{\left(L+\frac{\Delta l}{2}\right)^2-\left(x-\frac{\Delta l}{2}\right)^2}-\sqrt{L^2-x^2}\right]. \quad [25]$$

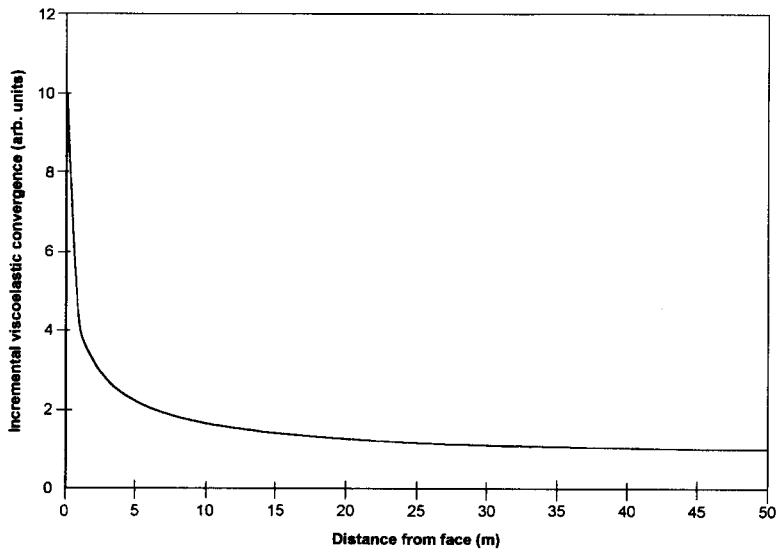

Figure 8—The incremental viscoelastic convergence as a function of the distance of the measuring instrument from the face

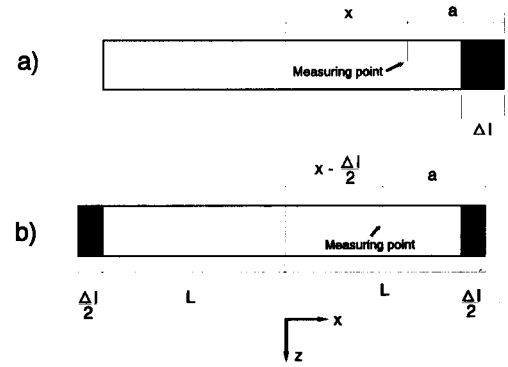

Figure 9—The equivalent stope principle

As an illustration of the method of parameter calibration, data from a longwall stope with a span of 200 m were used[15]. The depth of excavation was 2700 m, the dip was 25 degrees, and the closure instrument was installed 16,6 m from the face. After the blast (one side only), the increase in span was 1,4 m. For the purpose of comparison, the best fit obtainable by use of McGarr's empirical approach (equation [3]) for a relaxation constant of $\tau = 12$ and $\tau = 2$ is given in Figure 10.

It is clear that the empirical equation can be successfully calibrated only for either the primary or the secondary phase, giving a trade-off between the amount of initial information and the accurate long-term prediction. To illustrate the improvement obtained from the viscoelastic approach, equation [25] was fitted to the data by use of a spreadsheet and modification of the parameters to give the best fit. When the data are fitted, the following requirements need to be satisfied.

- It follows from the Kelvin model that q_0 and q_1 are positive. Parameters a_1 and a_2 must therefore also be positive.
- If a_1 and a_2 are positive, then $a_1 < a_2$ from equations [10] and [11].

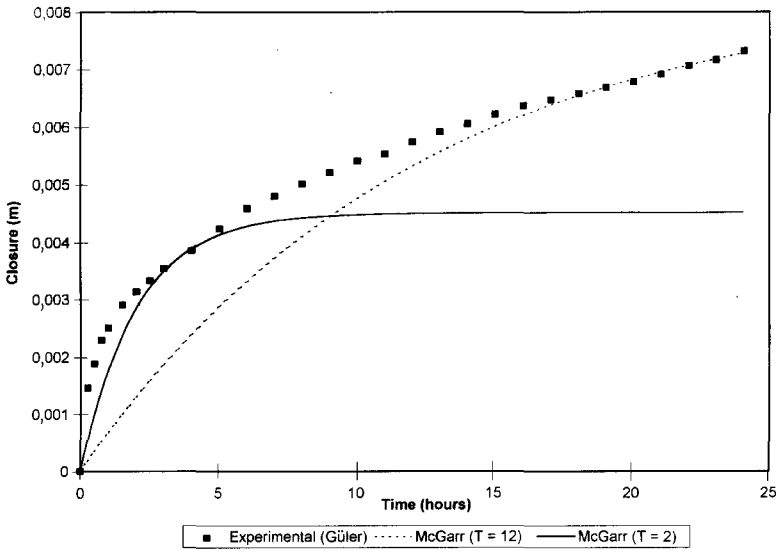

Figure 10—A comparison between experimental stope closure (Güler [15]) and the best fit obtainable from McGarr's empirical approach[17]

2. RYDER, J.A., and NAPIER, J.A.L. Error analysis and design of a large scale tabular mining analyser. *Proceedings 5th International Congress on Numerical Methods in Geomechanics.* Nagoya, 1985. pp. 1549–1555.
3. CROUCH, S.L. Computer simulation of mining in faulted ground. *J. S. Afr. Inst. Min. Metall.*, 1979. pp. 159–173.
4. COOK, N.G.W., HOEK, E., PRETORIUS, J.P.G., ORTLEPP, W.D., and SALAMON, M.D.G. Rock mechanics applied to the study of rockbursts. *J. S. Afr. Inst. Min. Metall.*, vol. 66. 1966. pp. 435–528.

- From equations [9] and [12], g must be positive and c_1 negative.
- It follows from equation [16] that c_1 must be smaller than –0,5; otherwise, Poisson's ratio will be negative.
- When a_1 and a_2 are calibrated, equation [18] must always be valid to ensure that the relationship between these time constants is maintained.

Figure 11 gives the experimental data (only the incremental part after the blast) and the fitted viscoelastic model. It is clear that a good fit can be obtained. The calibrated values for this stope are $g = 1{,}42 \times 10^{-5}$ Mpa^{-1}, $c_1 = -0{,}69$, $a_1 = 0{,}06$ h^{-1}, and $a_2 = 0{,}4$ h^{-1}. Equations [15], [16], and [17] can be used to give values for Young's modulus, Poisson's ratio, and the viscosity coefficient as $E = 65$ GPa, $\nu = 0{,}27$, and $q_1 = 850$ GPa·h.

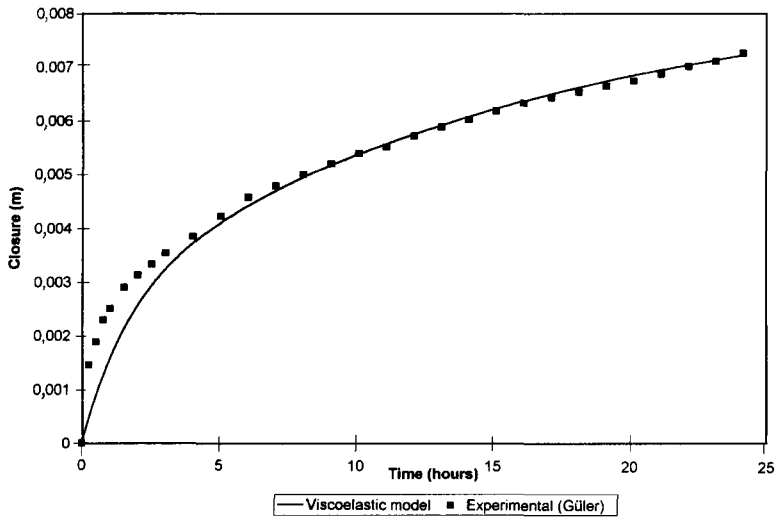

Figure 11—A comparison between experimental stope closure (Güler) and the best fit obtainable from the derived viscoelastic model

As an illustration of the practical use of this analysis, the long-term closure of the panel at this measuring point (if there is no further face advance) can be predicted by use of the calibrated values. The substitution of the value of g in equation [19] gives a closure of 209 mm. However, this calculation is valid only if the long-term closure at the centre of the stope is less than the stoping width. Again, this can be calculated by use of equation [19] with $x = 0$ and the calibrated value substituted for g. For this stope, the value at the centre is 380 mm, which is less than the stoping width of 1,2 m. Therefore, the calculation is valid.

Although it is possible by the use of this approach to represent transient stope closures, further work is necessary to quantify the contributions of the inelastic and time-dependent components to the closure. The different components contributing to the time-dependent component need to be separated so that the relative importance of each can be distinguished. As already mentioned, various workers have suggested that the gradual asymptotic closure in the secondary phase is caused by the time-dependent migration of the fracture zone ahead of the face. Further work is necessary to quantify this possible mechanism.

Conclusion

The viscoelastic approach can be used successfully to simulate observed stope closure. More accurate closure prediction is possible than by other known approaches, since the time-dependent components are included in the analysis. The advantage of the viscoelastic model over existing empirical methods is that it provides a better representation of both the primary and the secondary closure phases. This preliminary study showed that the representation of the rockmass as a Kelvin material is adequate. The use of more elaborate viscoelastic models must be weighed against the greater complexity of an increased number of parameters that need to be calibrated. However, further work is necessary to justify the assumption of Kelvin material. Care also needs to be exercised in the application of the derived viscoelastic model since it is not valid for stopes where total closure takes place and where the geometry is such that assumptions of plain strain are impossible. As most configurations in practice cannot be simplified to a two-dimensional approximation, further work is necessary to allow for three dimensions. This will have to take the form of numerical analysis to solve complex geometrical configurations.

5. ORTLEPP, W.D., and COOK, N.G.W. The measurement and analysis of the deformation around deep, hard rock excavations. *Proceedings 4th International Conference on Strata Control and Rock Mechanics.* 1964. pp. 140–150.
6. RYDER, J.A., and OFFICER, N.C. An elastic analysis of strata movement observed in the vicinity of inclined excavations. *J. S. Afr. Inst. Min. Metall.*, vol. 64. 1964. pp. 219–244.
7. GÜRTUNCA, R.G., and ADAMS, D.J. Determination of the *in situ* modulus of the rockmass by the use of backfill measurement. *J. S. Afr. Inst. Min. Metall.*, vol. 91. 1991. pp. 81–88.
8. GÜRTUNCA, R.G., JAGER, A.J., ADAMS, D.J., and GONLAG, M. The *in situ* behaviour of backfill materials and the surrounding rockmass in South African gold mines. *Proceedings 4th International Symposium on Mining with Backfill.* Montreal (Canada), 1989.
9. HOEK, E., GRABINSKY, M.W., and DIEDERICHS, M.S. Numerical modelling for underground excavation design. *Trans. Instn Min. Metall.*, vol. 100. 1991. pp. A22–A30.
10. NAPIER, J.A.L. and HILDYARD, M.W. Simulation of fracture growth around openings in highly stressed brittle rock. *J. S. Afr. Inst. Min. Metall.*, vol. 92. 1992. pp. 159–168.
11. CURRAN, J.H., and CRAWFORD, A.M. Comparative study of creep in rock and its discontinuities. *Proc. 21st Symposium on Rock Mechanics.* Rolla (USA), 1980. pp. 596–603.
12. GÜRTUNCA, R.G. Results of a classified tailings monitoring programme at Vaal Reefs. *COMRO Int. Rep.*, no. 614. 1989.
13. LEEMAN, E.R. Some measurements of closure and ride in a stope of the East Rand Proprietary Mines. *Pap. Assoc. Min. Mngrs, S. Afr.*, vol. 1958–1959. 1958. pp. 385–404.

The value of the work described here is that it aids the understanding of the behaviour of rock surrounding deep-level excavations. The motivation behind the examination of detailed closure profiles is to provide a better understanding of closure mechanisms. If there is a possible correlation between the time constants in the data and face bursting, a system of early warning could be developed. McGarr[17] has already suggested that the relaxation constant in his empirical model can be used as a risk-assessment parameter in conjunction with energy release rates. Similarly, the primary and secondary time constants in the viscoelastic model should be investigated. To accomplish this, experimental work needs to be carried out to clarify the relation between time-dependent observations and the formation of fractures.

Addendum: Viscoelastic convergence functions

Viscoelastic solution for a tabular deposit in isotropic ground

If the excavation is tabular and the geometry does not change for a long distance along the long axes, the stope can be idealized as a two-dimensional problem. Using these assumptions, Salamon[20] calculated the elastic convergence of a parallel-sided panel without contact between the hangingwall and the footwall as

$$S_z(x) = \frac{-4(1-\nu^2)W_z}{E} \sqrt{l^2 - x^2}\,(1 + \frac{dx}{2}), \qquad [A1]$$

where

$$W_z = \frac{-\gamma H}{2}\left[(1+k) + (1-k)\cos 2\alpha\right] \qquad [A2]$$

$$d = \frac{\sin\alpha \cos\beta}{H} \qquad [A3]$$

and

$2l$ = span of the stope
γ = specific weight of the rock
H = depth below surface
k = ratio of horizontal to vertical stress
α = dip of the reef
β = angle between the x-axis and the dip.

The z-axis is perpendicular to the plane of the excavation and points towards the footwall. The two-dimensional section is taken perpendicular to the y-axis (Figure 3).

The correspondence principle states that a viscoelastic solution can be obtained from the elastic solution if the inverse Laplace transformation of the elastic solution is taken after the elastic constants E and ν are replaced by their Laplace transforms $\tilde{E}$ and $\tilde{\nu}$, and if the actual loads, also by their Laplace transforms[18]. $\tilde{E}$ and $\tilde{\nu}$, are given by

$$\tilde{E} = \frac{3\tilde{Q}''\tilde{Q}'}{2\tilde{P}''\tilde{Q}' + \tilde{Q}''\tilde{P}'} \qquad [A4]$$

$$\tilde{\nu} = \frac{\tilde{P}''\tilde{Q}' - \tilde{Q}''\tilde{P}'}{2\tilde{P}''\tilde{Q}' + \tilde{Q}''\tilde{P}'}, \qquad [A5]$$

where P' and Q' are operators describing the viscoelastic material in dilatation (no change in shape), and P'' and Q'' are operators describing the material in distortion (change of shape).

When [A1] is subjected to the correspondence principle,

$$\tilde{S}_z = \frac{-4(1-\tilde{\nu}^2)\tilde{W}_z}{\tilde{E}} \sqrt{l^2 - x^2}\,(1 + \frac{dx}{2}). \qquad [A6]$$

On the assumption that W_z does not change with time,

$$\tilde{W}_z(s) = \frac{W_z}{s}. \qquad [A7]$$

Substitution of equations [A4], [A5], and [A7] into [A6] and transforming back to the time domain gives

$$S_z(x,t) = -4W_z F(t)\sqrt{l^2 - x^2}\,(1 + \frac{dx}{2}), \qquad [A8]$$

where

$$F(t) = L^{-1}\left[\frac{\tilde{P}''^2\tilde{Q}' + 2\tilde{P}''\tilde{P}'\tilde{Q}''}{s\tilde{Q}''(2\tilde{P}''\tilde{Q}' + \tilde{P}'\tilde{Q}'')}\right]. \qquad [A9]$$

The symbol L^{-1} is used to signify the inverse Laplace transformation.

Solution for a two-parameter Kelvin model

If the rock behaves elastically in dilatation and is viscoelastic according to the two-parameter Kelvin model in distortion, it follows that[19]

$$\tilde{P}' = 1 \quad \tilde{P}'' = 1 \quad \tilde{Q}' = 3K \quad \tilde{Q}'' = q_0 + sq_1,$$

where q_0 and q_1 are coefficients in the differential equation describing the Kelvin material. Therefore, [A9] becomes

$$F(t) = L^{-1}\left[\frac{3K + 2q_0 + 2q_1 s}{s(q_0 + sq_1)\,(6K + q_0 + sq_1)}\right]$$

$$= \frac{2}{q_1} L^{-1}\left[\frac{\frac{3K + 2q_0}{2q_1} + s}{s\left(\frac{q_0}{q_1} + s\right)\left(\frac{6K + q_0}{q_1} + s\right)}\right]. \qquad [A10]$$

14. KERSTEN, R.W.O. Personal communication, unpublished data, Hartebeesfontein Gold Mine.
15. GÜLER, G. Personal communication, unpublished data, Deelkraal Gold Mine.
16. HODGSON, K. The behaviour of the failed zone ahead of a face, as indicated by continuous seismic and convergence measurements. *COMRO Res. Rep.* 31/61. Transvaal and Orange Free State Chamber of Mines Research Organization. 1967.
17. MCGARR, A. Stable deformation near deep-level tabular excavations. *J. Geophys. Res.*, vol. 76, no. 29. 1971. pp. 7088–7106.
18. FLÜGGE, W. *Visco-elasticity.* 2nd ed. New York, Springer-Verlag, 1975.
19. PAN, Y.W., and DONG, J.J. Time-dependent tunnel convergence. I. Formulation of the model. *Int. J. Rock Mech. Min. Sci.*, vol. 28. 1991. pp. 469–475.
20. SALAMON, M.D.G. Two-dimensional treatment of problems arising from mining tabular deposits in isotropic or transversely isotropic ground. *Int. J. Rock Mech. Min. Sci.*, vol. 5. 1968. pp. 159–185.
21. SALAMON, M.D.G., RYDER, J.A., and ORTLEPP, W.D. An analogue solution for determining the elastic response of strata surrounding tabular mining excavations. *J. S. Afr. Inst. Min. Metall.*, vol. 65. 1964. pp. 115–137.
22. KRAUS, H. *Creep analysis.* New York, John Wiley & Sons, 1980. p. 6.
23. JAEGER, J.C., and COOK, N.G.W. *Fundamentals of rock mechanics.* 3rd ed. London, Chapman and Hall, 1979. p. 320.

Finding the inverse Laplace transformation by partial fraction expansion gives

$$F(t) = \frac{3K + 2q_0}{q_0(6K + q_0)} - \frac{1}{2q_0} e^{-\frac{q_0}{q_1}t} - \frac{3}{12K + 2q_0} e^{-\frac{6K+q_0}{q_1}t} \quad [A11]$$

When [A11] is substituted into equation [A8],

$$S_z(x,t) = -4W_z\sqrt{l^2 - x^2}\left(1 + \frac{dx}{2}\right)g \left[1 + c_1 e^{-a_1 t} + c_2 e^{-a_2 t}\right], \quad [A12]$$

where

$$g = \frac{3K + 2q_0}{q_0(6K + q_0)} \quad [A12a]$$

$$a_1 = \frac{q_0}{q_1} \quad [A12b]$$

$$a_2 = \frac{6K + q_0}{q_1} \quad [A12c]$$

$$c_1 = -\frac{6K + q_0}{6K + 4q_0} \quad [A12d]$$

$$c_2 = -\frac{3q_0}{6K + 4q_0} \quad [A12e]$$

For the two-parameter Kelvin stope-convergence model at $t = 0$, $S_z(x,t) = 0$ because $[1 + c_1 + c_2] = 0$ from [A12d] and [A12e]. Therefore, $c_2 = -[c_1 + 1]$. Equation [A12] can then be expressed as

$$S_z(x,t) = -4W_z\sqrt{l^2 - x^2}\left(1 + \frac{dx}{2}\right)g \left[1 + c_1 e^{-a_1 t} - (c_1 + 1)e^{-a_2 t}\right]. \quad [A13]$$

Solution for a three-parameter solid

If the rock behaves elastically in dilatation and according to the three-parameter solid in distortion, it follows that[19]

$$\tilde{P}' = 1 \quad \tilde{P}'' = 1 + p_1 s \quad \tilde{Q}' = 3K \quad \tilde{Q}'' = q_0 + sq_1,$$

where p_1, q_0, and q_1 are coefficients in the differential equation describing the three-parameter solid. When this is substituted into [A9],

$$F(t) = L^{-1}\left[\frac{3K(1 + p_1 s)^2 + 2(1 + p_1 s)(q_0 + q_1 s)}{s(q_0 + sq_1)\{6K(1 + p_1 s) + (q_0 + q_1 s)\}}\right] = \frac{p_1(3Kp_1 + 2q_1)}{q_1(6Kp_1 + q_1)} L^{-1}\left[\frac{\left(\frac{1}{p_1} + s\right)\left(\frac{3K + 2q_0}{3Kp_1 + 2q_1} + s\right)}{s\left(\frac{q_0}{q_1} + s\right)\left(\frac{6K + q_0}{6Kp_1 + q_1} + s\right)}\right]. \quad [A14]$$

Finding the inverse Laplace transformation by partial fraction expansion gives

$$F(t) = \frac{3K + 2q_0}{q_0(6K + q_0)} + \frac{p_1 q_0 - q_1}{2q_0 q_1} e^{-\frac{q_0}{q_1}t} + \frac{3(p_1 q_0 - q_1)}{2(6Kp_1 + q_1)(6K + q_0)} e^{-\frac{6K+q_0}{6Kp_1+q_1}t} \quad [A15]$$

When [A15] is substituted into equation [A8],

$$S_z(x,t) = -4W_z\sqrt{l^2 - x^2}\left(1 + \frac{dx}{2}\right)g \left[1 + c_3 e^{-a_1 t} + c_4 e^{-a_3 t}\right], \quad [A16]$$

where

$$a_3 = \frac{6K + q_0}{6Kp_1 + q_1} \quad [A16a]$$

$$c_3 = \frac{q_0(p_1 q_0 - q_1)}{2(6Kp_1 + q_1)(3K + 2q_0)} \quad [A16b]$$

$$c_4 = \frac{3q_0(p_1 q_0 - q_1)}{2(6Kp_1 + q_1)(3K + 2q_0)}. \quad [A16c]$$

Parameters g and a_1 are already defined in [A12a] and [A12b]. The format of equation [A16] is therefore similar to [A12] with parameters a_2, c_1, and c_2 replaced by a_3, c_3, and c_4. This follows because the additional element of the three-parameter model is a spring with no time dependency. At time $t = 0$, equation [A16] becomes

$$S_z(x, t = 0) = -4W_z\sqrt{l^2 - x^2}\left(1 + \frac{dx}{2}\right)g \left[1 + c_3 + c_4\right]. \quad [A17]$$

Because $[1 + c_3 + c_4] \neq 0$, $S_z(x, t = 0) \neq 0$ and the three-parameter solid-convergence model therefore gives an instantaneous deformation at time $t = 0$ given by equation [A17]. ◆